Visual Neuroscience (1997), **14**, 981–987. Printed in the USA.

Callosally projecting neurons in the macaque monkey V1/V2 border are enriched in nonphosphorylated neurofilament protein

PATRICK R. HOF,[1,2,3] LESLIE G. UNGERLEIDER,[4] MICHELLE M. ADAMS,[1,4] MAREE J. WEBSTER,[4,5] RICARDO GATTASS,[6] DANA M. BLUMBERG,[1] AND JOHN H. MORRISON[1,2]

[1]Neurobiology of Aging Laboratories and Fishberg Research Center for Neurobiology, Mount Sinai School of Medicine, New York
[2]Department of Geriatrics and Adult Development, Mount Sinai School of Medicine, New York
[3]Department of Ophthalmology, Mount Sinai School of Medicine, New York
[4]Laboratory of Brain and Cognition, National Institute of Mental Health, Bethesda
[5]Stanley Foundation Research Program, National Institute of Mental Health Neuroscience Center at St. Elizabeth's, Washington D.C.
[6]Departamento de Neurobiologia, Instituto de Biofísica Carlos Chagas Filho, Universidade Federal do Rio de Janeiro, Rio de Janeiro 21941-900, Brasil

(RECEIVED December 23, 1996; ACCEPTED February 24, 1997)

Abstract

Previous immunohistochemical studies combined with retrograde tracing in macaque monkeys have demonstrated that corticocortical projections can be differentiated by their content of neurofilament protein. The present study analyzed the distribution of nonphosphorylated neurofilament protein in callosally projecting neurons located at the V1/V2 border. All of the retrogradely labeled neurons were located in layer III at the V1/V2 border and at an immediately adjacent zone of area V2. A quantitative analysis showed that the vast majority (almost 95%) of these interhemispheric projection neurons contain neurofilament protein immunoreactivity. This observation differs from data obtained in other sets of callosal connections, including homotypical interhemispheric projections in the prefrontal, temporal, and parietal association cortices, that were found to contain uniformly low proportions of neurofilament protein-immunoreactive neurons. Comparably, highly variable proportions of neurofilament protein-containing neurons have been reported in intrahemispheric corticocortical pathways, including feedforward and feedback visual connections. These results indicate that neurofilament protein is a prominent neurochemical feature that identifies a particular population of interhemispheric projection neurons at the V1/V2 border, and suggest that this biochemical attribute may be critical for the function of this subset of callosal neurons.

Keywords: Callosal projections, Cytoskeleton, Neurochemical coding, Neurofilament protein, Primate visual system

Introduction

Visual callosal projections have been traditionally implicated in various aspects of visual function, such as midline stereopsis and perceptual fusion of the visual hemifields, vergence and guidance eye movements, and color vision (Myers, 1962; Choudhury et al., 1965; Hubel & Wiesel, 1967; Berlucchi & Rizzolatti, 1968; Blakemore et al., 1983; Land et al., 1983; Livingstone & Hubel, 1984). Physiological studies in primates have demonstrated that the receptive fields of callosal projections are located in the vicinity of the vertical meridian (Hubel & Wiesel, 1967; Innocenti, 1986). In addition, it has been shown that the V1/V2 border contains a representation of the ipsilateral visual field (Payne, 1990; Olavarria, 1996), and that the callosal projections connect retinotopically similar locations of both hemispheres in a non-mirror-symmetric manner, and thus contribute to perceptual fusion at the midline by conveying inputs from the contralateral eye onto corresponding ipsilateral fields (Payne, 1994; Olavarria, 1996).

The excitatory properties of the visual callosal connections are well established, and while the morphologic and electrophysiologic properties of these neurons have been investigated (Toyama et al., 1969; Harvey, 1980; Voigt et al., 1988; Weisskopf & Innocenti, 1991; Vercelli et al., 1992; Vercelli & Innocenti, 1993; Houzel et al., 1994; Innocenti et al., 1994), their neurochemical characteristics have not been analyzed. Recent analyses have demonstrated that pyramidal neurons containing high somatodendritic levels of a major component of the neuronal cytoskeleton, nonphosphorylated neurofilament protein, exhibit striking region-specific distribution patterns in the monkey visual cortex (Campbell & Morrison, 1989; Hof & Morrison, 1995; Chaudhuri et al., 1996).

Reprint requests to: Patrick R. Hof, Neurobiology of Aging Laboratories, Box 1639, Mount Sinai School of Medicine, One Gustave L. Levy Place, New York, NY 10029-6574, USA.

In addition, tract-tracing analyses have shown that the proportion of neurofilament protein-immunoreactive neurons among long association projections, as well as in visual pathways, is highly heterogeneous (Campbell et al., 1991; Hof et al., 1995*a*, 1996; Nimchinsky et al., 1996). It has been proposed that differences in the neurochemical phenotype of neurons furnishing corticocortical connections may be related to the role of a given cortical pathway (Hof et al., 1995*a*, 1996).

To define further the neurochemical features of neurons participating in corticocortical pathways, and to assess the degree to which cellular neurochemical specialization may be related to certain physiologic aspects of sensory processing, we analyzed the distribution of neurofilament protein-immunoreactive neurons in a callosal visual projection in macaque monkeys following injections of retrograde tracers in the contralateral V1/V2 border. Preliminary data from this study have been reported in abstract form (Hof et al., 1995*b*).

Methods

Seven adult Rhesus monkeys (*Macaca mulatta*) were used in the present study. Materials from these animals were used in previous studies of the macaque visual system as well (Hof & Morrison, 1995; Hof et al., 1995*a*,*b*, 1996), and all experimental protocols were conducted within NIH guidelines for animal research and were approved by the Institutional Animal Care and Use Committee (IACUC) at both Mount Sinai School of Medicine and NIH. Animals were tranquilized with ketamine hydrochloride (25 mg/kg, i.m.), intubated, and maintained under halothane general anesthesia (0.5–1.5% as necessary in air), and strict sterile surgical conditions. They were placed for surgery in a custom designed large animal head holder and a craniotomy was performed over the cortical site. Injections (200 nl each) of 4% aqueous solutions of either Fast Blue (FB) or Diamidino Yellow (DY) were placed within the cerebral cortex using a 1-μl Hamilton microsyringe with a 24-gauge needle along the posterior margin of the lunate sulcus within the border between areas V1 and V2 (Fig. 1; 6–16 injections depending on the case), with special care to avoid spreading of the dye in the subcortical white matter. The location of the boundary between areas V2 and V1 was recognized from the surface vasculature, and the proper placement of the injections within the cortex was further confirmed on histological materials.

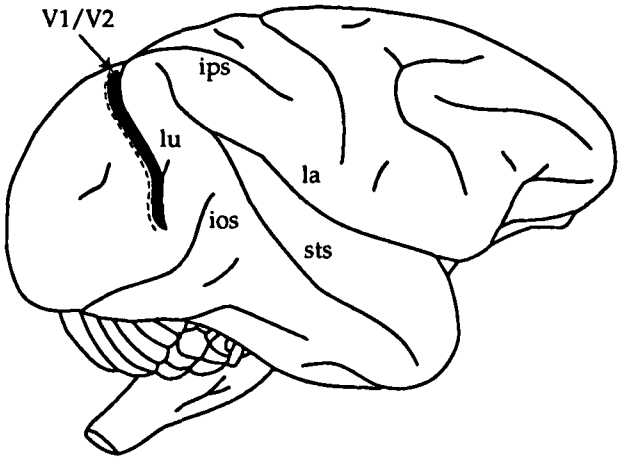

Fig. 1. Schematic representation of the lateral aspect of the macaque monkey brain showing the location of injection sites in the seven animals used in the present study. The posterior limit of the V1/V2 border is shown by a dashed line. Abbreviations: ios, inferior occipital sulcus; ips, intraparietal sulcus; la, lateral sulcus; lu, lunate sulcus; sts, superior temporal sulcus.

Following surgery, a survival time of 21 days was set to allow for reliable retrograde transport of FB and DY. Then, the animals were deeply anesthetized with ketamine hydrochloride (25 mg/kg, i.m.) and sodium pentobarbital (20–35 mg/kg, i.v., as necessary), intubated, and mechanically ventilated. The chest was opened to expose the heart, and 1.5 ml of 0.1% sodium nitrite was injected into the left ventricle. The descending aorta was clamped and the monkeys were perfused transcardially with cold 1% paraformaldehyde in phosphate buffer for 1 min followed by cold 4% paraformaldehyde for 10 to 12 min. The brains were then removed from the skull, cut into 4–10 mm thick coronal blocks, postfixed for 6 h in 4% paraformaldehyde at 4°C, and cryoprotected in sucrose. For histological and immunohistochemical purposes, the blocks were frozen on dry ice following postfixation and cryoprotection, and 40-μm-thick sections were cut from the coronal blocks on a cryostat. The sections from each block were kept in anatomical series and every tenth section was processed for immunohistochemistry. The remaining sections were cryoprotected and stored in serial order at −20°C (Hof & Morrison, 1995; Hof et al., 1995*a*,*b*, 1996; Nimchinsky et al., 1996).

Monoclonal antibody SMI-32 (Sternberger Monoclonals, Baltimore, MD), that recognizes nonphosphorylated epitopes on the medium (168 kDa) and heavy (200 kDa) molecular weight subunits of the neurofilament protein (Sternberger & Sternberger, 1983; Lee et al., 1988), was used in the present analysis. For immunohistochemistry, 40-μm-thick free-floating sections were incubated for 48 h at 4°C with this antibody at a dilution of 1:5,000 in phosphate-buffered saline containing 0.3% Triton X-100 and 0.5 mg/ml bovine serum albumin. The sections were then processed using a biotinylated secondary antibody and fluorescein-conjugated avidin D, mounted onto glass slides, and coverslipped with Permafluor. A parallel series of sections was stained for bright-field microscopy and processed with the avidin-biotin method using a Vectastain ABC kit (Vector Laboratories, Burlingame, CA) and 3,3′-diaminobenzidine as a chromogen, and intensified in 0.005% osmium tetroxide. Additional series of sections were stained with cresyl violet to clarify the cytoarchitecture and reconstruct the injection sites.

Analyses of the distribution of labeled neurons were performed using a computer-assisted image analysis system consisting of a Zeiss Axiophot photomicroscope equipped with a Zeiss MSP65 computer-controlled motorized stage (Zeiss, Oberkochen, Germany), a Zeiss ZVS-47E (Zeiss, Thornwood, NY) video camera system, a Macintosh 840AV workstation, and NeuroZoom morphometry software developed in collaboration with the Scripps Research Institute, La Jolla, CA (Nimchinsky et al., 1996; Young et al., 1996; Bloom et al., 1997). The numbers of retrogradely and double-labeled neurons projecting to the contralateral V1/V2 border were counted on digitized images in all immunostained sections. Neurons that were single labeled and double labeled (i.e. neurons containing the tracer only and containing the retrograde tracers and neurofilament protein immunoreactivity, respectively), were counted simultaneously by switching the filter combinations and superimposing the computer graphics on the monitor image. The position of each neuronal profile of interest was registered and labeled differently to assess the numbers of retrogradely labeled and double-labeled neurons. Accurate maps were electronically

constructed by assembling a series of microscopic fields to show the spatial distribution and regional clustering of labeled neurons in large areas (Hof et al., 1995*a*, 1996; Nimchinsky et al., 1996; Young et al., 1996). The *x*, *y*, *z* coordinates of each labeled neuron were recorded in each microscopic field relative to an origin, and the map was automatically assembled. Laminar boundaries were added by editing the map, and their accuracy was ascertained on adjacent sections stained with the antibody SMI-32 and on Nissl preparations (Fig. 2). The topographic localization of 2719 retrogradely labeled and 2571 double-labeled neurons was recorded in the present analysis. The data were calculated in each animal separately, due to variability in the number of retrogradely and double-labeled neurons among animals resulting from differences in the amount of tracers injected. However, the percentages of double-labeled neurons were consistent and were pooled across all animals. Possible differences in the percentages of double-labeled neurons among animals were assessed using a one-way analysis of variance.

Results

The distinct cytoarchitecture of the V1/V2 border has long been recognized in primates (OBγ, Von Economo, 1927), and is characterized in the macaque monkey by the presence of very large pyramidal neurons distributed over a few millimeters in the deep portion of layer III (Fig. 2). These neurons are in direct continuity with layer IVB of area V1 (Figs. 2A and 2C). In sections stained with antibody SMI-32, these giant pyramidal cells with extensive

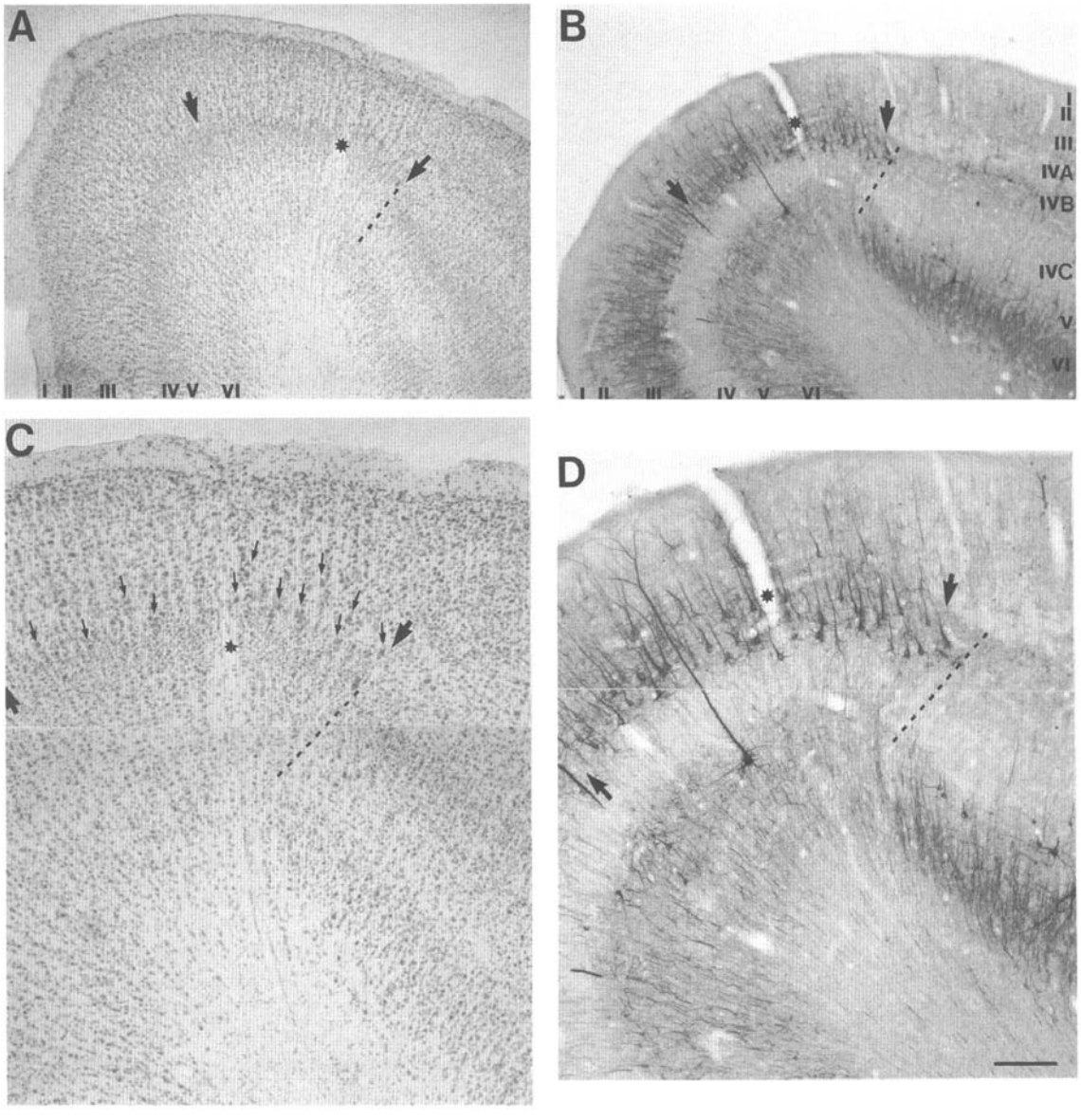

Fig. 2. Cytoarchitecture of the V1/V2 border. A, C: Nissl-stained section showing the presence of large neurons in layer III (thin arrows in C) that are continuous with layer IVB of area V1. B, D: Adjacent section stained with antibody SMI-32. Panels B and D are higher magnifications of the area shown in panels A and C, respectively. Note the very large neurofilament protein-immunoreactive pyramidal neurons clustered in the lower two-thirds of layer III (layer IIIb-c) at the boundary with area V1. Area V2 is to the left of the photomicrographs. The thick arrows indicate the limits of the V1/V2 border. The dashed lines show the limit of layer IV in area V1. Layers are identified by Roman numerals. Scale bar (on D) = 200 μm (A, B) and 100 μm (C, D).

apical and basal dendritic arborizations were intensely labeled and morphologically different from the neurons in layer IVB (Figs. 2B, 2D, 3A, 3C, and 3E). The number of neurofilament protein-immunoreactive neurons in layer III increased, while their somatic size progressively decreased, in area V2 (Hof & Morrison, 1995). Very rare immunoreactive neurons were observed in layer II, and layer IV was devoid of labeled cells. Layer V at the V1/V2 border exhibited very large, isolated neurofilament protein-containing pyramidal neurons (Figs. 2B and 2D). Small, very lightly stained pyramidal neurons were also present in layers V and VI, and polymorphic neurons were observed in layer VI. Layers V and VI of area V2 displayed staining patterns comparable to those at the V1/V2 border.

Following tracer injections of the contralateral V1/V2 border (Fig. 1), retrogradely labeled neurons were observed over the corresponding zone along the posterior margin of the lunate sulcus. As the injections were distributed along the entire extent of the V1/V2 border, retrogradely labeled neurons were visualized across most of the contralateral border (1747 neurons). Some labeling was also located in area V2 immediately over the crest of the lunate sulcus (874 neurons), and extending into V2 for about 5 mm, but none was observed in area V2 deeper in the lunate sulcus. In the V1/V2 border and in area V2, the retrogradely labeled neurons were generally grouped in small clusters, each containing 20 to 40 cells per section, that were larger in the V1/V2 border and smaller in V2. Rarely, retrogradely labeled cells were found in area V1 (98 neurons in all seven animals), in the vicinity of the V1/V2 border. It should be mentioned, however, that the localization and sparsity of these neurons in area V1 may be the result of slight deviations from the coronal plane during tissue processing and that they are in fact part of the V1/V2 border neuron population. The few retrogadely labeled neurons in area V1 were exclusively located in layer IIIc. At the V1/V2 border and in area V2, the retrogradely labeled neurons were located in layer III, the vast majority of them being confined to the lower two-thirds of this layer (layer IIIb-c; Figs. 3B, 3D, 3F, and 4). Layers II, V, and VI were completely devoid of retrogradely labeled neurons. These patterns matched closely those previously reported by other investigators (Myers, 1962; Pandya et al., 1971; Glickstein & Whitteridge, 1976; Spatz & Kunz, 1984; Kennedy et al., 1986; Gould et al., 1987; Meissirel et al., 1991; Olavarria & Abel, 1996).

The quantitative analysis of the projection neurons revealed that nearly all of the retrogradely labeled neurons contained neurofilament protein immunoreactivity at the V1/V2 border (2473 out of 2621 neurons, 94.4 ± 1.6%; Table 1; Figs. 3A–3F, and 4). Nearly all of the very large neurofilament protein-immunoreactive pyramidal neurons in layer IIIb-c at the V1/V2 border were retrogradely labeled. In addition, smaller immunoreactive neurons located in this layer also participated in this projection (Fig. 3). There was no statistically significant difference in the percentage of double-labeled neurons among the animals, although the individual counts of retrogradely labeled cells varied substantially (Table 1). Similar percentages of double-labeled cells were obtained from the neurons located at the V1/V2 border and in the region of area V2 immediately adjacent to it (Fig. 4). All of the rare callosally projecting neurons in layer IIIc of area V1 contained neurofilament protein.

Discussion

The present data indicate that, in macaque monkeys, the callosal projection from the V1/V2 border to the corresponding region of the contralateral hemisphere along the posterior aspect of the lunate sulcus is dominated by large layer III neurons that are enriched in nonphosphorylated neurofilament protein. The homogeneity of this projection in respect to neurofilament protein content is in contrast to the ipsilateral corticocortical projections interconnecting the prefrontal, limbic, temporal, parietal, and occipital cortices (Campbell et al., 1991; Hof et al., 1995*a*, 1996; Nimchinsky et al., 1996). Quantitative analyses using a similar experimental paradigm as in the present study have demonstrated that in subsets of visual corticocortical connections, a higher proportion of neurons projecting from areas V1, V2, V3, and V3A to area MT are neurofilament protein-immunoreactive (57–100%; of the projection neurons), than to area V4 (25–36%). In contrast, feedback projections from areas MT, V4, and V3 exhibit overall a consistent proportion of neurofilament protein-containing neurons (70–80%), regardless of their target in areas V1 or V2 (Hof et al., 1996). Interestingly, neurofilament protein immunoreactivity was found in 100% of the Meynert cells and layer IVB neurons participating in the projection linking area V1 to area MT (Hof et al., 1996). These results suggest that neurofilament protein identifies particular subpopulations of corticocortically projecting neurons with distinct regional and laminar distribution in the monkey visual system. In addition, long association pathways interconnecting the frontal, parietal, and temporal neocortex contain moderate to high numbers of neurofilament protein-immunoreactive pyramidal neurons (45–90% of the projection neurons), whereas short corticocortical, callosal, and limbic pathways are characterized by consistently fewer such neurons (4–35%; Campbell et al., 1991; Hof et al., 1995*a*; Nimchinsky et al., 1996). Among the commissural connections analyzed in a previous study, there are rather low percentages of double labeling (with a mean of 24.7 ± 3.6% for five commissural projections connecting homotopic cortical regions in the frontal, parietal, and temporal lobes [Hof et al., 1995*a*]), in sharp contrast with the present results.

The potential interactions among regional specialization, connectivity, and cellular characteristics such as neurochemical profile and morphology have been investigated recently in a series of experiments employing tract tracing of connections between the cingulate cortex and the primary motor cortex, cell loading of the retrogradely labeled neurons combined with cell reconstruction, subsequent immunohistochemistry, and confocal laser scanning microscopy to localize neurofilament protein in the identified neurons (Nimchinsky et al., 1996). This study demonstrated that these ipsilateral and commissural cingulate motor projection neurons displayed a high degree of morphologic heterogeneity, and no correlation could be found between somatodendritic morphology and presence of neurofilament protein. These data suggest that neurochemical phenotype represents a more important unifying characteristic of corticocortical neurons than morphology, at least in the case of these motor projections (Nimchinsky et al., 1996). This may not be entirely true of the callosal neurons at the V1/V2 border reported here, that show a much more consistent morphology than these cingulate motor neurons. However, the presence of a specialized cytoskeleton in the callosal projection from the V1/V2 border may also represent a key biochemical feature in these neurons which may be related to their specific role in the visual cortex, although no data are yet available to support directly such a correlation.

It has been proposed that neurofilament protein expression is neuron type-specific and contributes to the formation of the adult axonal and somatodendritic cytoskeleton (Riederer et al., 1995, 1996). It is involved in the maintenance and stabilization of the

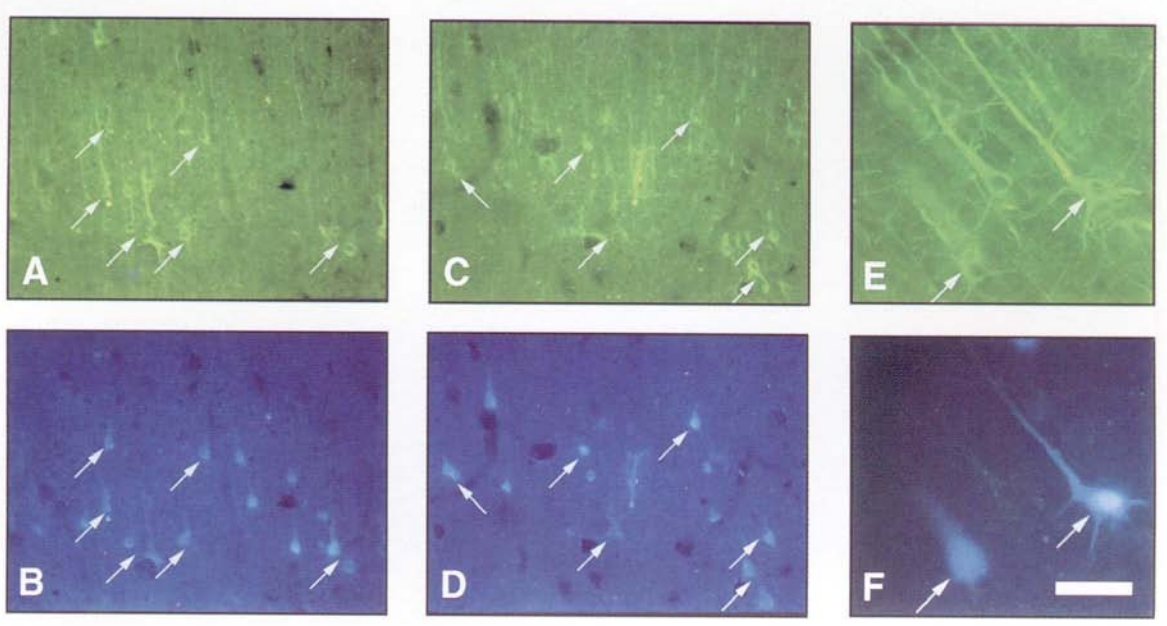

Figure 3

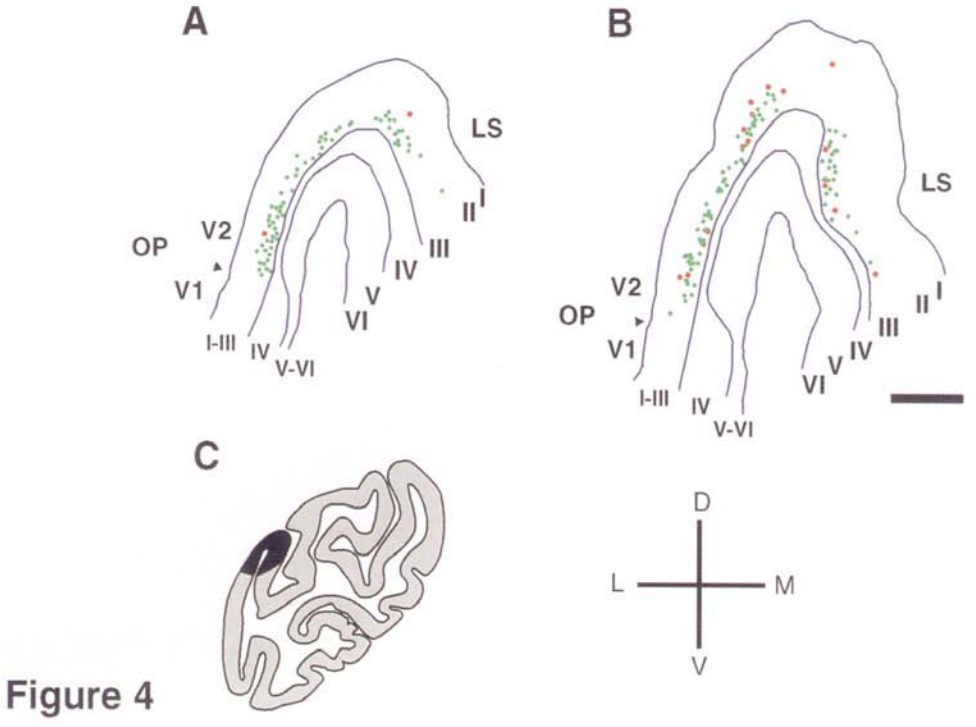

Figure 4

Fig. 3. Neurofilament protein-immunoreactive (A, C, E) and retrogradely labeled (B, D, F) callosally projecting neurons in layer IIIb-c at the V1/V2 border following Fast Blue injections in the contralateral hemisphere. Most of the retrogradely labeled neurons contain neurofilament protein immunoreactivity. Panels A–B, C–D, and E–F are pairs of photographs from the same microscopic field. The white arrows identify the same neurons in each pair of panels. Scale bar (on F) = 100 μm (A–D) and 50 μm (E, F).

Fig. 4. Representative computer-generated maps of the distribution of retrogradely labeled neurons (i.e. containing only the retrograde tracer; red squares) and double-labeled neurons (i.e. containing both the retrograde tracer and neurofilament protein immunoreactivity; green squares) at the V1/V2 border and immediately adjacent region of area V2 in the lunate sulcus (LS). Panels A and B are examples from different animals. Note that in both cases, the majority of the retrogradely labeled neurons contain neurofilament protein immunoreactivity. The maps were obtained from coronal sections and show only the posterior margin of the lunate sulcus and the dorsal portion of the opercular part of area V1 (OP). Comparable patterns were observed along the entire V1/V2 border. The arrowheads in A and B indicate the border between areas V1 and V2. Layers are identified by Roman numerals. Panel C shows a schematic representation of the region mapped in panels A and B (blackened zone of cortex) on a coronal section through the occipital lobe. Scale bar = 1 mm.

Table 1. *Quantitative analysis of callosally projecting neurofilament protein-immunoreactive neurons at the V1/V2 border*[a]

Monkey	9111	9415	9417	9501	9502	9503	9504
RL	107	243	321	486	537	345	582
DL	101	233	307	450	498	321	563
%	94.4	95.7	95.8	92.6	92.7	93.0	96.7

[a]Data show the numbers of retrogradely labeled neurons (RL; total number of neurons containing only the tracer) and of double-labeled neurons (DL; number of neurons containing both the tracer and neurofilament protein immunoreactivity), as well as the percent of double-labeled neurons (%) in each animal separately. Neurons were sampled from the V1/V2 border and from the immediately adjacent zone of area V2 near the lip of the lunate sulcus. In spite of variability in the number of labeled neurons, the percentages are remarkably consistent among animals, with a mean value of 94.4 ± 1.6%. All of these neurons were located in layer IIIb-c. Animal 9111, which exhibited substantially lower neuron counts, received fewer tracer injections.

axonal cytoskeleton, and its expression levels correlate with axonal size (Morris & Lasek, 1982; Hoffman et al., 1987; Nixon et al., 1994; Pijak et al., 1996; Xu et al., 1996). The presence of high levels of nonphosphorylated neurofilament protein in the somatodendritic compartment of subsets of neocortical neurons may be a neurochemical feature related to a distinctive role of these neurons in corticocortical systems (Campbell & Morrison, 1989; De Lima et al., 1990; Campbell et al., 1991; Hof & Morrison, 1995; Hof et al., 1995*a*, 1996; Nimchinsky et al., 1996). Of particular relevance is the fact that the presence of neurofilament protein in the neuron soma appears to be correlated to cell size and conduction velocity of nerve fibers (Lawson & Waddell, 1991). Interestingly, the neurons projecting from area V1 to area MT, that are characterized by high levels of neurofilament protein, are all very large and have large axons, up to 3 μm in diameter (Rockland, 1989, 1995), whereas short corticocortical connections are characterized by relatively lower levels of neurofilament protein immunoreactivity and originate from smaller neurons (Campbell et al., 1991; Hof et al., 1995*a*,*b*, 1996).

With respect to commissural connections, it is therefore possible that the projection neurons from the V1/V2 border are unique in the degree to which their biochemical phenotype (in this case a high somatodendritic level of nonphosphorylated neurofilament protein) is a defining characteristic of nearly all neurons participating in the projection. It should be kept in mind that the distribution of callosal connections in the primate visual system is not limited to the V1/V2 border, but that extensive sets of complex commissural projections exist in the prestriate cortex as well, that subserve additional roles such as completion of large receptive fields and interactions between field center and suppressive surrounds, and color constancy (Zeki, 1970; Van Essen et al., 1982; Antonini et al., 1983; Land et al., 1983; Maunsell & Van Essen, 1987; Spatz et al., 1987; Meissirel et al., 1991; Desimone et al., 1993). In view of the differences in neurofilament protein content among the callosal projection from the V1/V2 border and other interhemispheric connections, it will be interesting to extend the present neurochemical analysis to other callosal visual connections to investigate further the molecular characteristics of interhemispheric pathways as well as the potential role played by neurofilament protein in corticocortical projection neurons.

Acknowledgments

We thank C.A. Sailstad, W.G.M. Janssen, A.P. Leonard, and J.N. Sewell III for expert technical assistance; Dr. W.G. Young, S. González-Sherwin, and E.M. Gertz for software development; and Dr. E.A. Nimchinsky for critical reading of the manuscript. This work was supported in part by NIH Grants AG06647 and the Human Brain Project MHDA52154 (J.H.M.), the American Health Assistance Foundation (P.R.H.), and CNPq (R.G.).

References

Antonini, A., Berlucchi, G. & Lepore, F. (1983). Physiological organization of callosal connections of a visual lateral suprasylvian cortical area in the cat. *Journal of Neurophysiology* **49**, 902–921.

Berlucchi, G. & Rizzolatti, G. (1968). Binocularly driven neurons in visual cortex of split chiasm cats. *Science* **159**, 308–310.

Blakemore, C., Diao, Y., Pu, M., Wang, Y. & Xiao, Y. (1983). Possible function of the interhemispheric connexions between visual cortical areas in the cat. *Journal of Physiology* (London) **337**, 334–349.

Bloom, F.E., Young, W.G., Nimchinsky, E.A., Hof, P.R. & Morrison, J.H. (1997). Neuronal vulnerability and informatics in human disease. In *Progress in Neuroinformatics Research, Vol. 1, Neuroinformatics—An Overview of the Human Brain Project*, ed. Koslow, S.H. & Huerta, M.F., pp. 83–123. Mahwah, N.J.: Lawrence Erlbaum.

Campbell, M.J. & Morrison, J.H. (1989). Monoclonal antibody to neurofilament protein (SMI-32) labels a subpopulation of pyramidal neurons in the human and monkey neocortex. *Journal of Comparative Neurology* **282**, 191–205.

Campbell, M.J., Hof, P.R. & Morrison, J.H. (1991). A subpopulation of primate corticocortical neurons is distinguished by somatodendritic distribution of neurofilament protein. *Brain Research* **539**, 133–136.

Chaudhuri, A., Zangenehpour, S., Matsubara, J.A. & Cynader, M.S. (1996). Differential expression of neurofilament protein in the visual system of the vervet monkey. *Brain Research* **709**, 17–26.

Choudhury, B.P., Whitteridge, D. & Wilson, M.E. (1965). The function of the callosal connections of the visual cortex. *Quarterly Journal of Experimental Physiology* **50**, 214–219.

De Lima, A.D., Voigt, T. & Morrison, J.H. (1990). Morphology of the cells within the inferior temporal gyrus that project to the prefrontal cortex in the macaque monkey. *Journal of Comparative Neurology* **296**, 159–272.

Desimone, R., Moran, J., Schein, S.J. & Mishkin, M. (1993). A role for the corpus callosum in visual area V4 of the macaque. *Visual Neuroscience* **10**, 158–171.

Glickstein, M. & Whitteridge, D. (1976). Degeneration of layer III pyramidal cells in area 18 following destruction of callosal input. *Brain Research* **104**, 148–151.

Gould, H.J., III, Weber, J.T. & Rieck R.W. (1987). Interhemispheric connections in the visual cortex of the squirrel monkey (*Saimiri sciureus*). *Journal of Comparative Neurology* **265**, 14–28.

Harvey, A.R. (1980). A physiological analysis of subcortical and commissural projections of areas 17 and 18 of the cat. *Journal of Physiology* (London) **302**, 507–534.

Hof, P.R. & Morrison, J.H. (1995). Neurofilament protein defines regional patterns of cortical organization in the macaque monkey visual system: A quantitative immunohistochemical analysis. *Journal of Comparative Neurology* **352**, 161–186.

Hof, P.R., Nimchinsky, E.A. & Morrison, J.H. (1995*a*). Neurochemical phenotype of corticocortical connections in the macaque monkey: Quantitative analysis of a subset of neurofilament protein-immunoreactive projection neurons in frontal, parietal, temporal, and cingulate cortices. *Journal of Comparative Neurology* **362**, 109–133.

Hof, P.R., Ungerleider, L.G., Webster, M.J., Gattass, R., Adams, M.M., Sailstad, C.A., Janssen, W.G.M. & Morrison, J.H. (1995*b*). Feedforward and feedback corticocortical projections in the monkey visual system display differential neurochemical phenotype. *Society for Neuroscience Abstracts* **21**, 904.

Hof, P.R., Ungerleider, L.G., Webster, M.J., Gattass, R., Adams, M.M., Sailstad, C.A. & Morrison, J.H. (1996). Neurofilament protein is differentially distributed in subpopulations of corticocortical projection neurons in the macaque monkey visual pathways. *Journal of Comparative Neurology* **376**, 112–127.

Hoffman, P.N., Cleveland, D.W., Griffin, J.W., Landes, P.W., Cowan, N.J. &. Price, D.L. (1987). Neurofilament gene expression: A major

determinant of axonal caliber. *Proceedings of the National Academy of Sciences of the U.S.A.* **84,** 3472–3476.

HOUZEL, J.C., MILLERET, C. & INNOCENTI, G. (1994). Morphology of callosal axons interconnecting areas 17 and 18 of the cat. *European Journal of Neuroscience* **6**, 898–917.

HUBEL, D.H. & WIESEL, T.N. (1967). Cortical and callosal projections concerned with the vertical meridian of vertical visual fields in the cat. *Journal of Neurophysiology* **30**, 1561–1573.

INNOCENTI, G.M. (1986). General organization of callosal connections in the cerebral cortex. In *Cerebral Cortex, Vol. 5, Sensory-Motor Areas and Aspects of Cortical Connectivity*, ed. JONES, E.G. & PETERS A., pp. 291–355. New York: Plenum Press.

INNOCENTI, G.M., LEHMANN, P. & HOUZEL, J.C. (1994). Computational structure of visual callosal axons. *European Journal of Neuroscience* **6**, 918–935.

KENNEDY, H., DEHAY, C. & BULLIER, J. (1986). Organization of the callosal connections of visual areas V1 and V2 in the macaque monkey. *Journal of Comparative Neurology* **247**, 398–415.

LAND, E.H., HUBEL, D.H., LIVINGSTONE, M.S., PERRY, S.H. & BURNS, M.M. (1983). Colour-generating interactions across the corpus callosum. *Nature* **303**, 616–618.

LAWSON, S.N. & WADDELL, J.P. (1991). Soma neurofilament immunoreactivity is related to cell size and fibre conduction velocity in rat primary sensory neurons. *Journal of Physiology* (London) **435**, 41–63.

LEE, V.M.Y., OTVOS, L., JR, CARDEN, M.J., HOLLOSI, M., DIETZSCHOLD, B. & LAZZARINI, R.A. (1988). Identification of the major multiphosphorylation site in mammalian neurofilaments. *Proceedings of the National Academy of Sciences of the U.S.A.* **85**, 1998–2002.

LIVINGSTONE, M.S. & HUBEL, D.H. (1984). Anatomy and physiology of a color system in the primate visual cortex. *Journal of Neuroscience* **4**, 309–356.

MAUNSELL, J.H.R. & VAN ESSEN, D.C. (1987). Topographic organization of middle temporal visual area in the macaque monkey: Representational biases and the relationship to callosal connections and myeloarchitectonic boundaries. *Journal of Comparative Neurology* **266**, 535–555.

MEISSIREL, C., DEHAY, C., BERLAND, M. & KENNEDY, H. (1991). Segregation of callosal and association pathways during development in the visual cortex of the primate. *Journal of Neuroscience* **11**, 3297–3316.

MORRIS, J.R. & LASEK, R.J. (1982). Stable polymers of the axonal cytoskeleton: The axoplasmic ghost. *Journal of Cell Biology* **92**, 192–198.

MYERS, R.E. (1962). Commissural connections between occipital lobes of the monkey. *Journal of Comparative Neurology* **118**, 1–10.

NIMCHINSKY, E.A., HOF, P.R., YOUNG, W.G. & MORRISON, J.H. (1996). Neurochemical, morphologic and laminar characterization of cortical projection neurons in the cingulate motor areas of the macaque monkey. *Journal of Comparative Neurology* **374**, 136–160.

NIXON, R.A., PASKEVICH, P.A., SIHAG, R.K. & THAYER, C.Y. (1994). Phosphorylation on carboxyl terminus domains of neurofilament proteins in retinal ganglion cell neurons *in vivo*: Influences on regional neurofilament accumulation, interneuronal spacing, and axonal caliber. *Journal of Cell Biology* **126**, 1031–1046.

OLAVARRIA, J.F. (1996). Non-mirror-symmetric patterns of callosal linkages in areas 17 and 18 in cat visual cortex. *Journal of Comparative Neurology* **366**, 643–655.

OLAVARRIA, J.F. & ABEL, P.F. (1996). The distribution of callosal connections correlates with the pattern of cytochrome oxidase stripes in visual area V2 of macaque monkeys. *Cerebral Cortex* **6**, 631–639.

PANDYA, D.N., KAROL E.A. & HEILBROM, D. (1971). The topographic distribution of interhemispheric projections in the corpus callosum of the rhesus monkey. *Brain Research* **32**, 31–43.

PAYNE, B.R. (1990). Representation of the ipsilateral visual field in the transition zone between areas 17 and 18 of the cat's cerebral cortex. *Visual Neuroscience* **4**, 445–474.

PAYNE, B.R. (1994). Neuronal interactions in cat visual cortex mediated by the corpus callosum. *Behavioural Brain Research* **64**, 55–64.

PIJAK, D.S., HALL, G.F., TENICKI, P.J., BOULOS, A.S., LURIE, D.I. & SELZER, M.S. (1996). Neurofilament spacing, phosphorylation, and axon diameter in regenerating and uninjured lamprey axons. *Journal of Comparative Neurology* **368**, 569–581.

RIEDERER, B.M., DRABEROVA, E., VIKLICKY, V. & DRABER, P. (1995). Changes of MAP2 phosphorylation during brain development. *Journal of Histochemistry and Cytochemistry* **43,** 1269–1284.

RIEDERER, B.M., PORCHET, R. & MARUGG, R.A. (1996). Differential expression and modification of neurofilament triplet proteins during cat cerebellar development. *Journal of Comparative Neurology* **364,** 704–717.

ROCKLAND, K.S. (1989). Bistratified distribution of terminal arbors of individual axons projecting from area V1 to middle temporal area (MT) in the macaque monkey. *Visual Neuroscience* **3,** 155–170.

ROCKLAND, K.S. (1995). Morphology of individual axons projecting from area V2 to MT in the macaque. *Journal of Comparative Neurology* **355,** 15–26.

SPATZ, W.B. & KUNZ, B. (1984). Area 17 of anthropoid primates does participate in visual callosal connections. *Neuroscience Letters* **48**, 49–53.

SPATZ, W.B., KUNZ, B. & STEFFEN, H. (1987). A new heterotopic callosal projection of primary visual cortex in the monkey, *Callithrix jacchus*. *Brain Research* **403**, 158–161.

STERNBERGER, L.A. & STERNBERGER, N. (1983). Monoclonal antibodies distinguish phosphorylated and nonphosphorylated forms of neurofilaments *in situ*. *Proceedings of the National Academy of Sciences of the U.S.A.* **80**, 6126–6130.

TOYAMA, K., MATSUNAMI, K. & OHNO T. (1969). Antidromic identification of association, commissural and corticofugal efferent cells in cat visual cortex. *Brain Research* **14**, 513–517.

VAN ESSEN, D.C., NEWSOME, W.T. & BIXBY, J.L. (1982). The pattern of interhemispheric connections and its relationship to extrastriate visual areas in the macaque monkey. *Journal of Neuroscience* **2**, 265–283.

VERCELLI, A. & INNOCENTI, G.M. (1993). Morphology of visual callosal neurons with different locations, contralateral targets or patterns of development. *Experimental Brain Research* **94**, 393–404.

VERCELLI, A., ASSAL, F. & INNOCENTI, G.M. (1992). Emergence of callosally projecting neurons with stellate morphology in the visual cortex of the kitten. *Experimental Brain Research* **90**, 346–358.

VOIGT, T., LEVAY, S. & STAMNES, M.A. (1988). Morphological and immunocytochemical observations on the visual callosal projections in the cat. *Journal of Comparative Neurology* **272**, 450–460.

VON ECONOMO, C. (1927). *L'Architecture Cellulaire Normale de l'Écorce Cérébrale*. Paris: Masson.

WEISSKOPF, M. & INNOCENTI, G.M. (1991). Neurons with callosal projections in visual areas of newborn kittens: An analysis of their dendritic phenotype with respect to the fate of the callosal axon and of its target. *Experimental Brain Research* **86**, 151–158.

XU, Z., MARSZALEK, J.R., LEE, M.K., WONG, P.C., FOLMER, J., CRAWFORD, T.O., HSIEH, S.T., GRIFFIN, J.W. & CLEVELAND, D.W. (1996). Subunit composition of neurofilaments specifies axonal diameter. *Journal of Cell Biology* **133,** 1061–1069.

YOUNG, W.G., MORRISON, J.H., HOF, P.R., NIMCHINSKY, E.A. & BLOOM, F.E. (1996). NeuroZoom—Topographical mapping and stereological counting, distribution of data, and collaborative computing. *Society for Neuroscience Abstracts* **22**, 1238.

ZEKI, S.M. (1970). Interhemispheric connections of prestriate cortex in monkey. *Brain Research* **19**, 63–75.